

---

---

**ORIGINAL ARTICLE**

---

---

# **Metal Artefact Reduction for Orthopaedic Devices Using Monoenergetic Extrapolation from Dual-energy Computed Tomography**

**JCY Lee, CK Shiu, KC Lai, MK Chan**

*Department of Radiology and Imaging, Queen Elizabeth Hospital, Jordan, Hong Kong*

## **ABSTRACT**

**Objectives:** To assess the diagnostic performance and clinical efficacy of metal artefact reduction using monoenergetic imaging with dual-energy computed tomography (DECT).

**Materials:** A total of 30 patients with 32 metal device regions were examined using the DECT protocol with 100 kVp and 140 kVp spectra. Specific post-processing software was used to generate optimised monoenergetic images and standard combined images by filtered back projection. Two independent observers subjectively graded the degree of artefact and diagnostic quality of the two sets of images on a five-point rating scale. The beam-hardening artefact (mean density of the most pronounced streak 1 cm from the device) was compared between both groups. Qualitative assessment by type of device (internal or external device) was performed.

**Results:** A total of 32 examinations with 19 internal, 10 external, and 3 internal + external implanted metal devices were performed. Monoenergetic imaging was rated superior for artefact reduction in 75% cases and for diagnostic quality in 78% cases, compared with standard combined imaging by filtered back projection ( $p < 0.001$ ). The mean density of beam hardening artefacts improved from -725.22 HU in standard combined imaging to -519.02 HU using monoenergetic imaging ( $p = 0.025$ ). The presence of an external metal device adversely affected the artefact reduction performance of monoenergetic imaging ( $p = 0.045$ ), without significantly affecting diagnostic quality.

**Conclusion:** Monoenergetic extrapolation using DECT can significantly reduce metal artefact and improve diagnostic quality compared with filtered back projection. Its performance was adversely affected by the presence of an external device.

**Key Words:** Artifacts; Diagnostic imaging; Radiography, dual-energy scanned projection; Tomography, X-ray computed

## **中文摘要**

### **使用單能量外推法在雙能量電腦斷層掃描時減少骨科矯形裝置的金屬物偽影**

李俊賢、蕭俊傑、黎國忠、陳文光

**目的：**評估使用雙能量電腦斷層掃描（DECT）的單能量成像來減少金屬物偽影的診斷性能和臨床

---

**Correspondence:** Dr Jonan Chun-yin Lee, Department of Radiology and Imaging, Queen Elizabeth Hospital, Jordan, Kowloon, Hong Kong  
Email: jonanleecy@gmail.com

Submitted: 12 Apr 2016; Accepted: 23 Jun 2016.

Disclosure of Conflicts of Interest: All authors have disclosed no conflicts of interest.

效果。

**材料：**30名裝上32個金屬裝置的患者接受100 kVp和140 kVp光譜的DECT檢查。使用特別後處理軟件來濾波反投影並產生優化單能量成像和標準組合圖像。兩個獨立的觀察者用五點評分量表去比較這兩組圖像的診斷質量和金屬物偽影程度，包括束硬化偽影（距離裝置1cm的最明顯條紋的平均密度）。根據內部矯形裝置或外部矯形裝置進行了定性評估。

**結果：**共32次檢查包括19個內部、10個外部和3個內部+外部金屬植入物。與濾波反投影標準組合成像相比，75%單能量成像被評定為較能減少偽影，而78%單能量成像被評定為有較佳診斷質量（ $p < 0.001$ ）。束硬化偽影的平均密度從標準組合成像中的-725.22HU改善至單能量成像中的-519.02HU（ $p = 0.025$ ）。外部金屬裝置的存在不利於單能量成像偽影的減少（ $p = 0.045$ ），但不顯著影響診斷。

**結論：**與濾波反投影相比，使用DECT的單能外推法可顯著減少金屬偽影並提高診斷質量，但其性能會受到外部金屬裝置的不利影響。

## INTRODUCTION

Since the use of computed tomography (CT) in musculoskeletal imaging, metallic artefacts have been a significant limiting factor in image quality and diagnostic evaluation of metallic implants, bone-implant interface, and adjacent soft tissues.<sup>1,2</sup> These metallic artefacts are a result of beam hardening,<sup>3,4</sup> photon starvation,<sup>5</sup> and scatter artefacts.<sup>6</sup> CT has been suboptimal in visualising both metal-to-bone interfaces (that requires higher energy) and the adjacent soft tissue detail (that requires lower energy).<sup>7</sup>

The introduction of dual-energy CT (DECT) enables a reduction in metal artefacts.<sup>8</sup> Prior to the introduction of dual-source CT, this could be achieved with a single-source DECT scanner with fast kilovoltage switching. Nonetheless, spectral separation is limited between high- and low-energy scans, resulting in higher noise levels at a lower peak voltage.<sup>7,9</sup> The introduction of dual-source CT enables more effective use of dual energy and improves spectral separation and equalisation of dose and noise between high- and low-energy scans using tube current modulation.

With dual-source DECT, CT attenuation coefficients are measured simultaneously using two energy spectra (e.g. 100 kVp and 140 kVp). A single set of images is then generated for diagnostic purposes. This can be achieved by either traditional filtered back projection (FBP) to produce a standard combined image, or by monoenergetic extrapolation. Using a linear computation equation, monoenergetic images of

different energy quanta can be generated in the image domain, as if created by a wide spectrum of energy level.<sup>10</sup> By selecting the optimal energy (in keV), metal artefacts can be minimised for diagnostic evaluation. In some cases, additional diagnostic findings may only be apparent after monoenergetic reconstruction.<sup>11</sup>

DECT allows dose-neutral acquisition at 100 kV and 140 kV simultaneously. It provides a wide range of energy settings (50 to 190 keV) for users to achieve the optimal level for substantial metal artefact reduction. The monoenergetic images synthesised from the image data domain can reduce beam-hardening artefacts and enhance diagnostic quality.

This study aimed to assess the diagnostic performance and clinical efficacy of metal artefact reduction using monoenergetic imaging with DECT, and compare it with standard combined image by FBP.

## METHODS

The study was approved by the institutional ethics committee. Informed patient consent was not required as it was a retrospective study.

### Patient population

We retrospectively reviewed the hospital record of 17 males and 13 females aged 21 to 100 (mean, 55.6; standard deviation, 20.2) years who underwent CT examination of a metal device in an upper extremity ( $n = 3$ ), lower extremity ( $n = 27$ ), or trunk ( $n = 2$ ) between February 2014 and February 2015.

## Implant Location, Types, and Material

The medical device included an internal metallic implant ( $n = 19$ ), external metallic implant ( $n = 10$ ), or both ( $n = 3$ ). Location, number, and type of metal implant are shown in Table 1. In our institution, the orthopaedic implants are typically made of 316L stainless steel (iron, chromium, and nickel). Occasionally, 'super-metal' alloys (e.g. cobalt-chromium-molybdenum) and titanium alloys are also used.

## Imaging Protocol, Image Post-processing and Analysis

DECT examinations were performed with a dual-source CT scanner (SOMATOM Definition Flash, Siemens Medical, Forchheim, Germany) using two tube voltages of 100 kVp and 140 kVp. Post-processing was performed on a commercially available workstation with specific software (Syngo workplace, Siemens Healthcare, Forchheim, Germany). Images were reconstructed into two datasets: average-weighted FBP images with decomposition of 0.5 (50% density information from 100 kVp, 50% from 140 kVp) and optimised monoenergetic images. The optimal energy setting for monoenergetic extrapolation was obtained between 100 and 150 (median, 138) keV and chosen by a trained radiographer who verified the image. The mean  $\pm$  SD volume computed tomography dose index was  $15.6 \pm 3.2$  mGy. The mean  $\pm$  SD dose length product was  $529.3 \pm 255.6$  mGy\*cm. Images were reformatted

with slice thickness and interval of 3 mm. A specific dose-reduction protocol with automated tube current modulation (CARE Dose 4D, Siemens, Forchheim, Germany) was turned on in all examinations. The monoenergetic images were then compared with standard combined images from FBP. Image qualitative and quantitative assessment was performed on the AGFA Picture Archiving and Communication System (IMPAX 6.4.0, AGFA Healthcare, Mortsels, Belgium).

## Qualitative Assessment

All examination datasets were anonymised. The images of all datasets were independently reviewed by two observers (with 4 and 6 years' experience in radiology) who were blinded to clinical information, examination details, prior imaging findings and reports, as well as the other observer's score. All images were reviewed on the axial plane in bone window setting (Window Width 1500, Window Level 450). The degree of artefact and diagnostic quality of images were subjectively graded on a five-point rating scale (Table 2).<sup>12</sup>

## Quantitative Assessment

The beam-hardening artefact, quantified as the artefact attenuation in Hounsfield units (HU) of the most pronounced streak 1cm from the device, was measured in both datasets. A circular region of interest measuring 23-25 mm<sup>2</sup> was placed in the same area of the same image section. Reference density measurement was obtained in similar soft tissue outside the areas of artefact.

## Statistical Analysis

Statistical analysis was performed by SPSS (Statistical Package for the Social Sciences, version 22.0). Wilcoxon signed-rank test was used to compare the subjective grading of artefacts and diagnostic quality of imaging methods. Mann-Whitney  $U$  test was used to compare the beam-hardening artefacts and the effect by type of metallic device.

**Table 1.** Location and type of metal implant.\*

Location	Internal implant	External implant	Internal + external implants	Total
Lower extremity	15	9	3	27
Upper extremity	3	0	0	3
Trunk	1	1	0	2
<b>Total</b>	<b>19</b>	<b>10</b>	<b>3</b>	<b>32</b>

\* There are 6 screws, 7 plates and screws, 4 prostheses, 7 intramedullary nails, and 13 external fixators.

**Table 2.** Subjective grading for metallic artefacts and diagnostic quality.<sup>12</sup>

Score	For metallic artefacts	For diagnostic quality
0	Absence of artefacts	Fully diagnostic
1	Minor streaks only at the thickest portion of the metallic implant	Minor artefacts in areas of thick metal that do not affect diagnostic evaluation
2	Minor streaks without significant obscuration of area of interest	Minor streaks without impact on the evaluation of the implant and the adjacent tissue
3	Pronounced streaks obscuring a large area of interest	Restricted diagnostic interpretation; reduced diagnostic confidence
4	Massive artefacts obscuring almost the entire area of interest	Severely impaired diagnostic interpretability; exclusion or inclusion of pathology significantly affected

**Table 3.** Qualitative and quantitative image quality assessment.

Variable	Monoenergetic	Filtered back projection	p Value
Diagnostic quality score	2.1 ± 1.2	3.2 ± 0.8	<0.001
Artefact score	2.3 ± 1.2	3.2 ± 0.7	<0.001
Artefact density (Hounsfield units)	-519.0 ± 407.7	-725.2 ± 303.7	0.025
Reference soft tissue density (Hounsfield units)	48.3 ± 15.4	48.8 ± 14.7	0.898

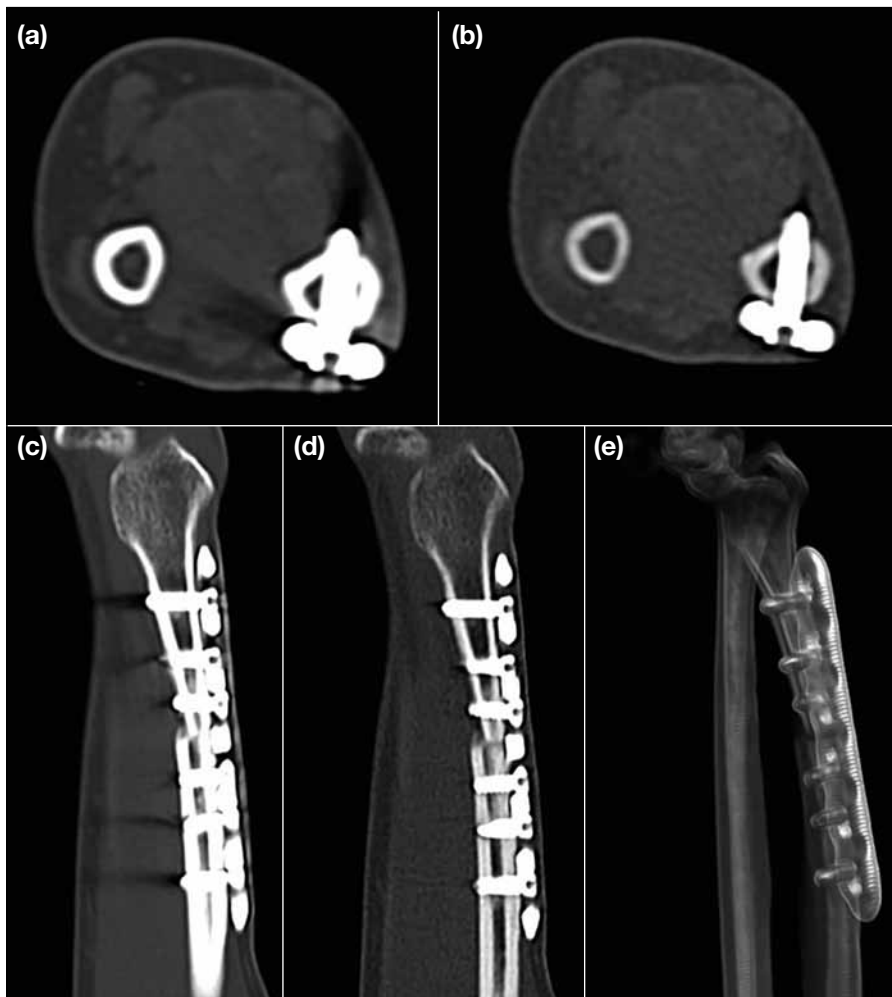


**Figure 1.** (a, b) Axial and (c, d) sagittal reformatted images of the radius after open reduction and internal fixation using filtered back projection and monoenergetic extrapolation. Note the reduced streak artefacts and discernible bone implant interface in the monoenergetic image. (e) The 3D volume-rendering image using dual-energy computed tomography data set.

Cohen's kappa coefficient was used to measure the agreement between two observers. Kappa values of 0.61-0.80 were interpreted as substantial and 0.81-1.00 as excellent agreement. P values <0.05 were regarded as statistically significant.

## RESULTS

### Qualitative and Quantitative Assessment

The subjective image quality was better in monoenergetic images than in FBP images in terms of diagnostic score (2.1 ± 1.2 vs. 3.2 ± 0.8,  $p < 0.001$ ) and artefact score (2.3 ± 1.2 vs. 3.2 ± 0.7,  $p < 0.001$ ) [Table 3].

Monoenergetic images were rated superior for artefact reduction in 24/32 (75%) cases and for diagnostic quality in 25/32 (78%) cases, compared with average-weighted FBP imaging (Figure 1).

Inter-observer agreement between the two readers for the degree of artefact and diagnostic quality was substantial to excellent, with a Kappa coefficient ranging from 0.623 to 0.850.

The mean density of the most pronounced streak was strongly negative in both imaging protocols. With the

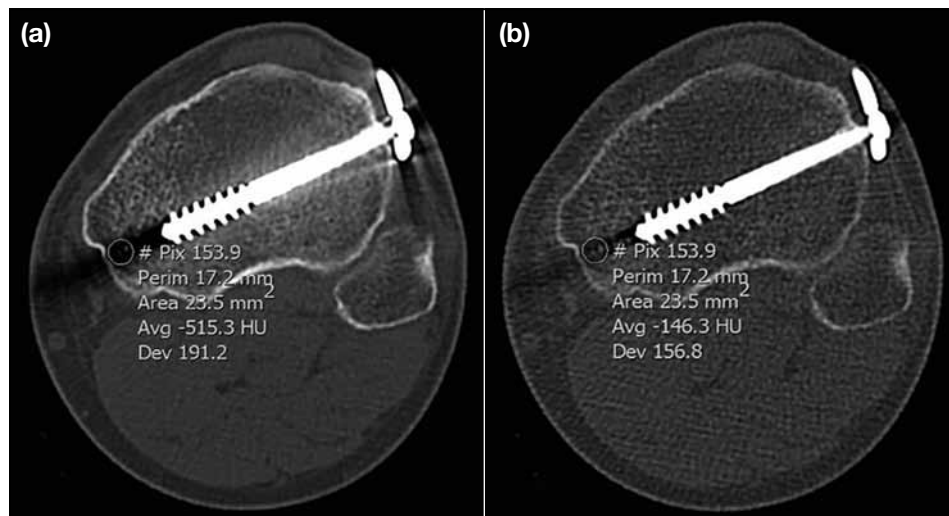


**Figure 2.** The attenuation coefficient measured in Hounsfield Units (HU) was  $-515.3 \pm 191.2$  HU for (a) standard filtered back projection image and  $-146.3 \pm 156.8$  HU for (b) monoenergetic extrapolation image.

**Table 4.** Artefact and diagnostic scores by type of device.

Score	Monoenergetic	Filtered back projection	$\Delta$ Mean
Artefact score			( $p = 0.045$ )
Internal	$2.00 \pm 1.38$	$3.01 \pm 0.77$	$1.05 \pm 0.73$
External / internal+external	$2.73 \pm 0.60$	$3.42 \pm 0.58$	$0.69 \pm 0.55$
Diagnostic quality score			( $p = 0.864$ )
Internal	$1.89 \pm 1.45$	$2.97 \pm 0.88$	$1.08 \pm 0.85$
External / internal+external	$2.50 \pm 0.58$	$3.54 \pm 0.51$	$1.03 \pm 0.53$

use of monoenergetic DECT, the absolute value of HU of the most pronounced streak increased from  $-725.2$  to  $-519.0$  ( $p = 0.025$ , Table 3), therefore producing quantitatively less artefacts (Figure 2). The reference soft tissue densities were consistent between the two protocols.

### Qualitative Assessment by Types of Device

The presence of an external metallic device adversely affected the artefact reduction performance of monoenergetic DECT without affecting diagnostic quality (Table 4). A large external metallic device caused photon starvation that might not be corrected using monoenergetic extrapolation (Figure 3).

## DISCUSSION

CT plays a crucial role in postoperative follow-up of implant-related problems including malunion, infection, aseptic loosening, osteolysis, dislocation, and periprosthetic fracture.<sup>7</sup> Metallic artefacts from beam hardening can significantly impair image quality, making it unsuitable for diagnostic purposes.<sup>13</sup>

Various methods for metal artefact reduction are

available but there are compromises. Increasing the tube current and voltage or decreasing collimator size can reduce artefacts but increase radiation dose.<sup>14</sup> Iterative frequency split-normalised metal artefact reduction<sup>15</sup> or other iterative metal artefact reduction<sup>16</sup> have also been proposed, but are expensive.

DECT has been of great interest to musculoskeletal radiologists for metal artefact reduction.<sup>17</sup> DECT decreases artefact density by utilising both low energy and high energy, resulting in superior image quality compared with conventional CT imaging.<sup>12,18</sup> It can be achieved without an increase in total radiation dose.<sup>7,8,10,18</sup>

After generating two sets of data of different energies from DECT, a single set of images is generated during post-processing following image reconstruction. It can be achieved by monoenergetic extrapolation instead of standard FBP. Monoenergetic reconstructions are easy to apply during post-processing and can result in superior image quality.<sup>14,19,20</sup>

Our study confirmed that monoenergetic DECT can

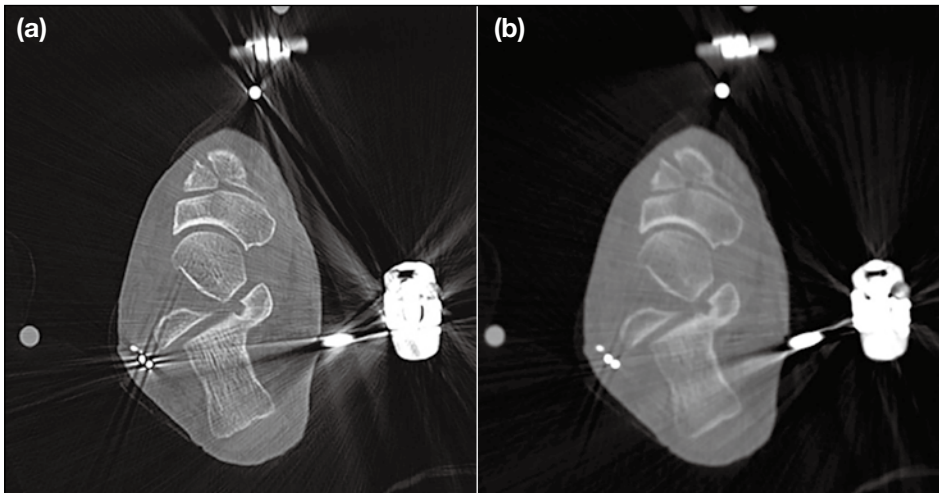


**Figure 3.** Thick metallic streaks are present in (a) filtered back projection image and (b) monoenergetic extrapolation image. The large external metallic device causes photon starvation that cannot be corrected using monoenergetic extrapolation.

reduce metal artefacts in vivo. To the best of our knowledge, this is the first local study performed on clinical cases to compare the usefulness of monoenergetic imaging with traditional FBP. The results are consistent with those of other international studies, and can contribute towards further large-scale systematic reviews.

The presence of an external metallic device was a significant factor in successful artefact reduction, although the overall diagnostic confidence was still improved when compared with FBP. This is because other factors, alongside metal artefacts, including photon starvation and nonlinear partial volume averaging, adversely affect the performance of DECT for metal artefact reduction. Another metal reduction technique, e.g. iterative reconstruction, may be more helpful, and a comparison of these two methods would be useful.

Our study results were limited by the small sample size. Recruiting a higher number of subjects over a longer period would increase the statistical power. A large cohort, multi-centred study is warranted.

In our study, the optimal energy settings were decided after image acquisition. The criteria for optimal energy selection was not standardised and might have varied with individual operators. It would also have required additional time and manpower. It is possible to set a standard energy setting<sup>12</sup> that range between 105 and 141 keV, depending on imaged anatomical region, composition and size of the metal implant.<sup>2</sup> One study found no significant difference between 105 keV and

individual optimal energy setting, thereby implying that reconstruction can be routinely carried out at 105 keV without the need for individual optimisation.<sup>12</sup> Nonetheless, in a human cadaveric study, a chosen monoenergetic value of 120 keV worked best for a certain type of metallic plate at the proximal humerus.<sup>2</sup> In a local in-vitro study using a phantom body, optimal monoenergetic energy level differed based on the implant type and material used.<sup>21</sup> Further large-scale clinical trials in patients are needed to optimise the protocol in this respect. A standardised optimal energy (in keV) may therefore be tailor-made based on an institution's preference, type of metallic device, and imaged region. This may accelerate workflow and improve efficiency, but will require further local experience.

## CONCLUSION

Monoenergetic extrapolation using DECT can reduce metal artefacts and improve diagnostic quality in the evaluation of implant-related complications, compared with standard FBP. Its performance is adversely affected by the presence of an external metallic device, although the diagnostic confidence is still higher.

## REFERENCES

1. Lee MJ, Kim S, Lee SA, Song HT, Huh YM, Kim DH, et al. Overcoming artifacts from metallic orthopedic implants at high-field-strength MR imaging and multi-detector CT. *Radiographics*. 2007;27:791-803. [cross ref](#)
2. Winklhofer S, Benninger E, Spross C, Morsbach F, Rahm S, Ross S, et al. CT metal artefact reduction for internal fixation of the proximal humerus: value of mono-energetic extrapolation from dual-energy and iterative reconstructions. *Clin Radiol*. 2014;69:e199-206. [cross ref](#)

3. Haramati N, Staron RB, Mazel-Sperling K, Freeman K, Nickoloff EL, Barax C, et al. CT scans through metal scanning technique versus hardware composition. *Comput Med Imaging Graph.* 1994;18:429-34. [crossref](#)
4. Barrett JF, Keat N. Artifacts in CT: recognition and avoidance. *Radiographics.* 2004;24:1679-91. [crossref](#)
5. Watzke O, Kalender WA. A pragmatic approach to metal artifact reduction in CT: merging of metal artifact reduced images. *Eur Radiol.* 2004;14:849-56. [crossref](#)
6. Boas FE, Fleischmann D. Evaluation of two iterative techniques for reducing metal artifacts in computed tomography. *Radiology.* 2011;259:894-902. [crossref](#)
7. Pessis E, Campagna R, Sverzut JM, Bach F, Rodallec M, Guerini H, et al. Virtual monochromatic spectral imaging with fast kilovoltage switching: reduction of metal artifacts at CT. *Radiographics.* 2013;33:573-83. [crossref](#)
8. Johnson TR, Krauss B, Sedlmair M, Grasruck M, Bruder H, Morhard D, et al. Material differentiation by dual energy CT: initial experience. *Eur Radiol.* 2007;17:1510-7. [crossref](#)
9. Kaza RK, Platt JF, Cohan RH, Caoili EM, Al-Hawary MM, Wasnik A. Dual-energy CT with single- and dual-source scanners: current applications in evaluating the genitourinary tract. *Radiographics.* 2012;32:353-69. [crossref](#)
10. Coupal TM, Mallinson PI, McLaughlin P, Nicolaou S, Munk PL, Ouellette H. Peering through the glare: using dual-energy CT to overcome the problem of metal artefacts in bone radiology. *Skeletal Radiol.* 2014;43:567-75. [crossref](#)
11. Meinel FG, Bischoff B, Zhang Q, Bamberg F, Reiser MF, Johnson TR. Metal artifact reduction by dual-energy computed tomography using energetic extrapolation: a systematically optimized protocol. *Invest Radiol.* 2012;47:406-14. [crossref](#)
12. Bamberg F, Dierks A, Nikolaou K, Reiser MF, Becker CR, Johnson TR. Metal artifact reduction by dual energy computed tomography using monoenergetic extrapolation. *Eur Radiol.* 2011;21:1424-9. [crossref](#)
13. Park HS, Chung YE, Seo JK. Computed tomographic beam-hardening artefacts: mathematical characterization and analysis. *Philos Trans A Math Phys Eng Sci.* 2015;373(2043).
14. Zhou C, Zhao YE, Luo S, Shi H, Li L, Zheng L, et al. Monoenergetic imaging of dual-energy CT reduces artifacts from implanted metal orthopedic devices in patients with fractures. *Acad Radiol.* 2011;18:1252-7. [crossref](#)
15. Morsbach F, Bickelhaupt S, Wanner GA, Krauss A, Schmidt B, Alkadhi H. Reduction of metal artifacts from hip prostheses on CT images of the pelvis: value of iterative reconstructions. *Radiology.* 2013;268:237-44. [crossref](#)
16. Yu L, Li H, Mueller J, Kofler JM, Liu X, Primak AN, et al. Metal artifact reduction from reformatted projections for hip prostheses in multislice helical computed tomography: techniques and initial clinical results. *Invest Radiol.* 2009;44:691-6. [crossref](#)
17. Runge VM. Advances in diagnostic radiology. *Invest Radiol.* 2010;45:823-6. [crossref](#)
18. Yu L, Leng S, McCollough CH. Dual-energy CT-based monochromatic imaging. *AJR Am J Roentgenol.* 2012;199(5 Suppl):S9-S15. [crossref](#)
19. Lewis M, Reid K, Toms AP. Reducing the effects of metal artefact using high keV monoenergetic reconstruction of dual energy CT (DECT) in hip replacements. *Skeletal Radiol.* 2013;42:275-82. [crossref](#)
20. Wang Y, Qian B, Li B, Qin G, Zhou Z, Qiu Y, et al. Metal artifacts reduction using monochromatic images from spectral CT: evaluation of pedicle screws in patients with scoliosis. *Eur J Radiol.* 2013;82:e360-6. [crossref](#)
21. Chan WC, Tsang JP, Wong WY, Chu PY, To VY, Lee CY, et al. Metal artefact reduction by dual-energy computed tomography using monoenergetic extrapolation: in-vitro determination of optimal monoenergetic level with different metallic implants using a phantom body. *Hong Kong J Radiol.* 2016;19:35-42. [crossref](#)